39th AIAA/ASME/SAE/ASEE
Joint Propulsion Conference and Exhibit
July 20-23, 2003, Huntsville, AL

Paper 2003-4820

WAVE IMPLOSION AS AN INITIATION MECHANISM FOR PULSE DETONATION ENGINES

S.I. Jackson, M.P. Grunthaner and J.E. Shepherd
Graduate Aeronautical Laboratories,
California Institute of Technology, Pasadena, CA 91125

A device has been developed which uses shock focusing to enhance the transmission efficiency of an initiator tube when used with pulse detonation engines. The initiator is capable of initiating detonations in ethylene-air and propane-air mixtures using less initiator fuel than is used in a conventional initiator tube. This toroidal initiator uses a single spark and an array of small-diameter channels to generate and merge many detonation waves to create a single detonation wave with a toroidal front. The collapsing front generates a high-temperature and pressure focal region. This region of high energy density is used to facilitate more efficient transmission of the detonation wave from the initiator into the fuel-air mixture.

The development of this device was detailed in previous work (Jackson, S.I. and Shepherd, J.E., "Initiation Systems for Pulse Detonation Engines," AIAA Paper 2002–3627, July 2002). The following describes modifications made to the device to allow for its use with pulse detonation engines. Results presented include temporal history of pressure near the focus of the collapsing torus and images of the front luminosity. The critical amount of initiator gas required to detonate propane-air and ethylene-air mixtures is then discussed. Finally, the overall efficiency of the toroidal initiator is compared to other initiation mechanisms such as spherical initiation, planar initiation, and initiator tubes.

Nomenclature

A_{tube}	Cross-sectional area of tube
B	Constant
c	Sound speed
c_{CJ}	Sound speed at Chapman-Jouguet conditions
d	Main (test section) tube inner diameter
d_d	Initiator tube inner diameter
E_a	Activation energy
E_c	Critical energy for initiation
$E_{d,corr}$	Corrected initiator energy
$E_{d,uncorr}$	Uncorrected initiator energy
E_j	Blast initiation energy (geometry specific)
E_s	Blast wave initiation energy
$E^*_{cylindrical}$	Critical energy for cylindrical initiation
E^*_{planar}	Critical energy for planar initiation
$E^*_{spherical}$	Critical energy for spherical initiation
$E_{toroidal}$	Energy of toroidal initiator
j	geometry index (1 for planar, 2 for cylindrical, 3 for spherical)
L	Characteristic length of DDT
L_d	Initiator tube length
M_{CJ}	Chapman-Jouguet detonation wave Mach number
M_s	Instantaneous Mach number of shock wave
M^*_s	Critical shock Mach number
P	Instantaneous pressure
P_0	Initial pressure
P_{CJ}	Pressure at Chapman-Jouguet condition
$\tilde{R}$	Universal gas constant
R_0	Explosion length
R^*_s	Critical shock radius
R^*_s	Instantaneous radius of shock wave
$R^*_{cylindrical}$	Critical shock radius for cylindrical initiation
R^*_{planar}	Critical shock radius for planar initiation
$R^*_{spherical}$	Critical shock radius for spherical initiation
t_c	Chemical time-scale
T_s	Post-shock temperature
U_{CJ}	Chapman-Jouguet detonation wave velocity
V_d	Volume of simple tube initiator

$V_{toroidal}$	Volume of toroidal initiator
Δ	Reaction zone thickness based on peak energy release
Δh^0	Effective heat of reaction of mixture
γ	Ratio of specific heats in mixture
λ	Cell size
θ	Reduced activation energy
ρ	Density
ρ_0	Initial density
τ	Induction time
τ_{CJ}	Induction time at Chapman-Jouguet conditions

Introduction

THE development of efficient methods of initiating detonations in insensitive hydrocarbon-air mixtures (such as JP10-air or C_3H_8-air) is essential to the success of pulse detonation engines. Existing pulse detonation engines[1,2] use a tube initiator to initiate hydrocarbon-air mixtures. The tube initiator contains a sensitive mixture such as propane-oxygen that transitions to a detonation in a very short distance after ignition by a weak spark. The fully developed detonation wave in the initiator is then propagated into the insensitive hydrocarbon-air mixture. If the transmitted shock Mach number and the post-shock flow duration are sufficient,[3] the detonation wave will be successfully transmitted into the hydrocarbon-air mixture.

Current tube initiator technology has several drawbacks. Typically, the tube initiator is located in the center of the detonation tube, resulting in drag as air flows through the device. Furthermore, use of a tube initiator as an initiator for pulse detonation engines requires an amount of energy to be stored on-board during flight. This energy can be either stored electrically in batteries and capacitors or thermodynamically in a sensitive initiator mixture. Given the state of current technology, it is more efficient to store the energy on-board in the form of an initiator mixture carrying only enough battery power to periodically ignite the mixture with a weak spark.

While the initiator mixture is lighter than large banks of batteries, the stored gas still takes up payload weight and results in engine performance losses. Thus, it is critical that the tube initiator use as little gas as possible in order to maximize the engine performance. To reduce the amount of initiator gas, it is necessary to increase the efficiency of the tube initiator. One way to increase initiator efficiency is to use shock focusing.

In shock focusing, a collapsing shock wave generates a high-pressure and high-temperature focal region by adiabatically compressing shocked gas as it flows into an ever-decreasing area.[4] This compression is capable of generating regions of extremely high energy density. It is also possible to apply shock focusing concepts to detonation waves to generate high-pressure and high-temperature regions.[5–11] Compressing the detonation products increases the post-detonation wave pressure higher than the Chapman-Jouguet (CJ) pressure, resulting in an increasingly overdriven detonation wave.

Thus, shock focusing can be used to increase the overpressure of the shock transmitted from the initiator section into the engine, which has been shown to increase the transmission efficiency.[12] This technique is dependent only on the geometry of the initiator wave and provides the means to dramatically increase the transmission efficiency or to reduce the amount of initiator gas used.

Murray et al.[12] noted an increase in transmission efficiency when the detonation in the initiator was transmitted into the detonation tube through an annular orifice. They reasoned that the annular orifice generated an imploding toroidal wave in the test section. The high pressure and temperature at the focus of the imploding toroid created a region of high energy density that was capable of evolving into a self-sustaining detonation wave. In particular, they noted that the inclusion of the annular orifice allowed successful detonation transmission for tubes with diameters 2.2 times smaller than tubes with simple circular orifices.

Research at Caltech extended this concept using a sensitized initiator gas in an effort to increase transmission efficiency. Using this technique, detonations were realized in C_3H_8-air mixtures at room temperature (298 K). It was not possible to initiate detonations at elevated temperatures (373 K) in the C_3H_8-air or JP10-air mixtures. This loss in performance was attributed to the decrease in energy density of the initiator and test gas mixtures due to gas expansion during heating. Thus, recent research[13] has involved developing a more efficient focusing technique that is capable of achieving detonations in the hydrocarbon-air mixtures of interest at elevated temperatures.

For the past three years, Caltech has been involved in a program to develop an imploding toroidal wave capable of initiating detonations in hydrocarbon-air mixtures with a single low-energy spark (less than 100 mJ) for use in short-length (less than 1 m), small-diameter (76 mm) detonation tubes. A strong detonation wave is generated by deflagration-to-detonation transition (DDT) in a sensitive fuel-oxygen mixture initiated with a low-energy (less than 30 mJ) electrical spark. The detonation creates an annular shock or detonation wave, which is shaped into a collapsing torus that implodes at the axis of symmetry of the main detonation tube. Previous work has characterized the imploding wave[5,13] and focused on the technique used to efficiently develop an imploding wave from a single spark.[13] Use of an imploding wave as an initiation mechanism is also appealing because the initiator can be incorporated into the detonation tube walls. Thus, no part of the initiator is located in the air flow path,

reducing drag losses typically associated with tube initiators.

The present work describes the further development of these shock focusing techniques for pulse detonation engine applications. Imploding detonations and shock waves were used to initiate hydrocarbon-air mixtures. Experimental parameters involved varying the amount of initiator gas necessary for successful initiation and the wall proximity to the focusing event. A blast wave solution for spherical and planar critical initiation energies[14] and a model for predicting initiator dimensions[3] are used to demonstrate the increased efficiency of the shock focusing initiator when compared to more straightforward initiation methods such as spherical initiation and initiation by a simple tube initiator.

Initiator Development

The typical cycle for a pulse detonation engine that uses a sensitized tube initiator to detonate hydrocarbon-air mixtures is as follows. The main tube is filled with the fuel-air mixture. Concurrently or shortly thereafter, the tube initiator is filled with the sensitized mixture. A detonation is then initiated in the tube initiator and passes into the main tube. The combustion products exhaust from the main tube, generating thrust. After a brief purge time to allow the combustion products to vent, the cycle is repeated. Ideally, the cycle is repeated 60-100 times a second in order to generate a quasi-steady thrust that is comparable to that produced by current turbine engines. Cycle frequencies of 60-100 hertz correspond to cycle periods of 10-17 ms. This time is a key consideration in designing initiator systems but has not been addressed in the present study.

In operating previously designed initiators[13] under this cycle, it became apparent that design flaws existed such that rapidly filling the initiator with the initiator mixture was not possible. Therefore, it was necessary to modify the initiator design in order to accommodate rapid gas injection. The design and operation of the "first-generation" of initiators is briefly reviewed. Problems with the first-generation design are highlighted and corrected leading to a "second-generation" design. The results of these second-generation initiators are then presented.

Previous Work

Previously, a device capable of producing a 15 cm by 18 mm planar detonation wave from a single spark was successfully built and tested.[13] This planar initiator was intended to demonstrate the principles of merging a series of wave fronts into a single front. The method of wave merging is similar to techniques used in high explosive research.[15]

This first-generation planar initiator, shown in Figure 1, consists of a main channel with secondary channels branching off the main channel. All secondary channels terminate on a line and exhaust into a common test section area. The channel geometry is such that all path lengths from the spark pointing to the secondary channel termination line are equal.

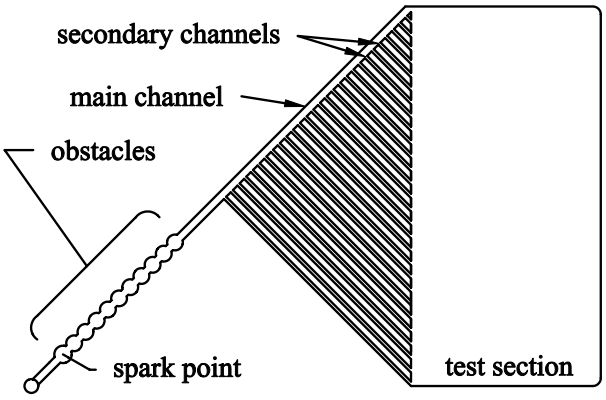

Fig. 1 Planar initiator schematic.

During operation, all channels are filled with a detonable mixture. A spark plug and associated discharge system with 30 mJ of stored energy is used to ignite a deflagration in the mixture. The deflagration then undergoes DDT in the obstacle section. The result is a detonation wave that travels down the main channel with small fronts branching off and traveling down the secondary channels. All detonation fronts exhaust into the test section at the same time and combine to form a planar detonation front. A more detailed discussion of the device is available in previous work.[13]

To create an imploding wave, the planar initiator design is mapped onto a cylinder. The exit of each channel lies on a circle with the channels exhausting inwards. Thus, the device creates an imploding toroidal wave. The inner cylinder containing the channels is sealed against an outer sleeve using a shrink fit.[16] The toroidal initiator is capable of generating a repeatable imploding wave with a high-pressure focal region.[13]

Injection Problems

The first-generation initiator design was not suitable for rapid filling of the initiator channels. Different paths through the device had different flow resistance. The varying flow resistance with path choice is attributed to (1) the difference in dimensions in the main and secondary channels and (2) the presence of the secondary channel entrances on the main channel wall. The result was that gas injected at the spark point flowed through the main channel much more easily than through the secondary channels. This effect is illustrated using water channel experiments with dye in Figure 2.

During these experiments, gas injected into the initiator travels preferentially down the main channel. Small channels near the end of the main channel fill more quickly than those at the beginning. Thus, detonation waves do not travel through the device in a

regular and repeatable manner, resulting in a non-planar wave. In order for the injected gas to uniformly fill the device, it was necessary to redesign the channel geometry such that the channel resistance was independent of path length.

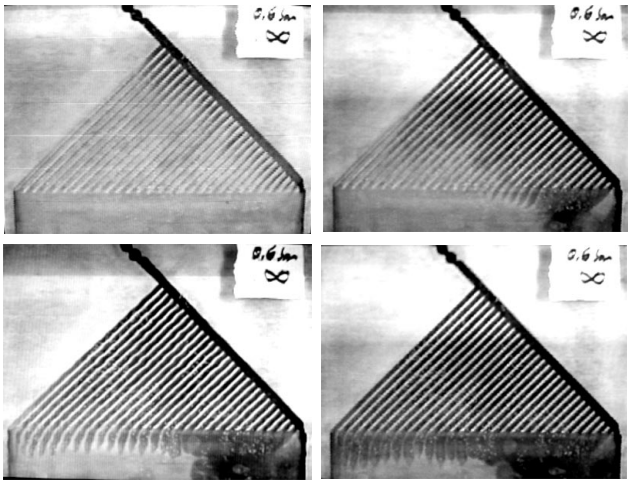

Fig. 2 Water colored with dye was injected into the planar initiator from a 0.6 bar gauge source. Note how the injected fluid fills the main channel more quickly than the smaller channels. The planar initiator is oriented 90° clockwise compared to the schematic shown in Fig. 1.

Second-Generation Design

The new channel geometry is shown in Figure 3. As with previous devices, the distance from the spark point to the end of the secondary channels is the same. However, the geometry now also ensures that each path through the device has the same flow resistance.

Planar Initiator

The planar initiator is shown in Figure 3. The overall dimensions of the device shown in Figure 3 are 26 cm by 56.5 cm (10.3 in by 22.3 in). Gas is injected into the device through the hole located at the start of the main channel (left of Figure 3). The spark plug (not shown) is located next to this gas injection port. Just downstream of the gas injection port, a series of circular indentations have been milled into the main channel to promote DDT. Shortly after the obstacles, the main channel bifurcates into the next family of channels. There are five families of channels. Information on each set of channels is contained in Table 3. The last series of channels exhausts into a test section that is 15 cm in width and 51 mm in length. The height of the test section expands linearly from the height of the last series of channels to a final height of 18 mm over a distance of 67 cm. The final portion of the test section is equipped with three pressure transducers (PCB 113A2 series) spaced 5.72 cm apart. The transducers allow measurement of the time of arrival of the resulting planar wave. A polycarbonate window and 1 mm thick Teflon gasket seal the channels and provide optical access to the top of the initiator. The test section end of the initiator is attached to a 3.65 m long channel to make Caltech's narrow channel (18 x 150 mm) test facility.[17]

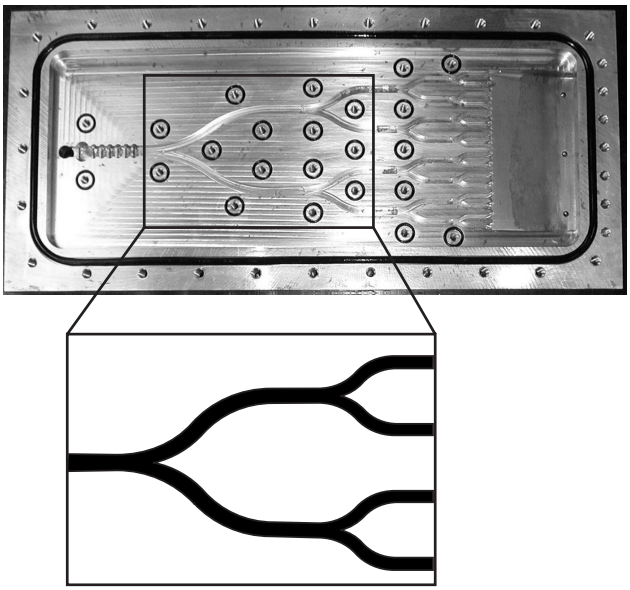

Fig. 3 The second planar initiator is shown. Note the symmetric channel design.

Family number	Number of channels	Channel width	Arc length per channel
1	1	10.2 mm	152.4 mm
2	2	8.53 mm	115.7 mm
3	4	7.19 mm	89.4 mm
4	8	6.05 mm	53.8 mm
5	16	5.08 mm	35.6 mm

Table 1 Channel dimensions of the second-generation planar initiator shown in Figure 3.

During testing, the initiator and test section are filled with the mixture to be studied using the method of partial pressures. Circulation of the gas mixture via a bellows pump ensures homogeneity of the test gas. Approximately one second before ignition, equimolar acetylene and oxygen gas is injected into the device just behind the spark plug. Injection continues for approximately 0.8 seconds until all initiator channels (but not the test section) are filled with the acetylene-oxygen mixture. When all channels are filled, the spark plug is fired, releasing about 30 mJ of stored energy into the initiator mixture. As in the previous design, the resulting deflagration rapidly accelerates into a detonation over the obstacle section in the first channel. The resulting detonation than branches out as it travels down successive channels. The detonation wavelets emerge from the small channels into the test section at the same time and combine to form a planar detonation, which is then propagated into the test section mixture.

Figure 4 contains a series of images taken by an

intensified CCD camera with exposure times of 100 ns. The channel orientation is the same as in Figure 3. Chemiluminescence of the burning gas allows the progress of the detonation to be traced throughout the initiator channels. In the final image, the detonations in the channels have combined in the test section to form the planar detonation front. Pressure traces from the test section indicate that the resulting front in the test section is planar to within 6 mm over a distance of 15 cm.

Toroidal Initiator

As with previous designs, the toroidal initiator was created by mapping the channel geometry of the planar initiator to a cylinder. The cylinder or "inner sleeve" containing the channels in the second-generation toroidal initiator is shown in Figure 5a. As in the previous design, this inner sleeve was shrunk by immersion in liquid nitrogen and inserted into another cylinder (outer sleeve). The dimensions of the cylinders were such that, at identical temperature, the outer diameter of the inner sleeve was slightly larger than the inner diameter of the outer sleeve. The result was a shrink fit between the two cylinders that acts to seal the channels. This technique is discussed in detail in previous work.[16] The outer array of channels surrounds a central tube with a diameter of 76 mm (3.0 in).

During initial testing, the toroidal initiator was filled with stoichiometric propane-oxygen or ethylene-oxygen mixtures using the method of partial pressures. As before, a bellows pump was used to recirculate the gas to ensure homogeneity. After recirculation, the spark was discharged. Pressure histories at different locations along the end flange were obtained. The resulting imploding wave was also imaged with an intensified CCD camera.

Four pressure transducers were mounted on a surface 19 mm from the center exit of the initiator as shown in Figure 5b. The transducers were spaced 10.7 mm apart on a radial line with the central transducer located on the central axis of the tube. A typical set of pressure traces is shown in Figure 6. The outermost three pressure transducers show a pressure wave amplitude that is consistent with the pressure predicted by classical CJ theory (P_{CJ}). However, the pressure transducer closest to the focus of the device measures pressures that are ten times P_{CJ}. Similar focal pressures have also been measured in earlier devices and by other researchers studying cylindrical imploding shock waves.[5–9]

In order to obtain optical access of the inside of the device, the end flange containing the pressure transducers was removed and replaced with a composite polycarbonate and glass window. Images were obtained with an intensified CCD camera placed a short distance outside this viewing window. A pressure transducer mounted near the exhaust of one of the secondary channels acted as a trigger. Unless mentioned, exposure times were 100 ns.

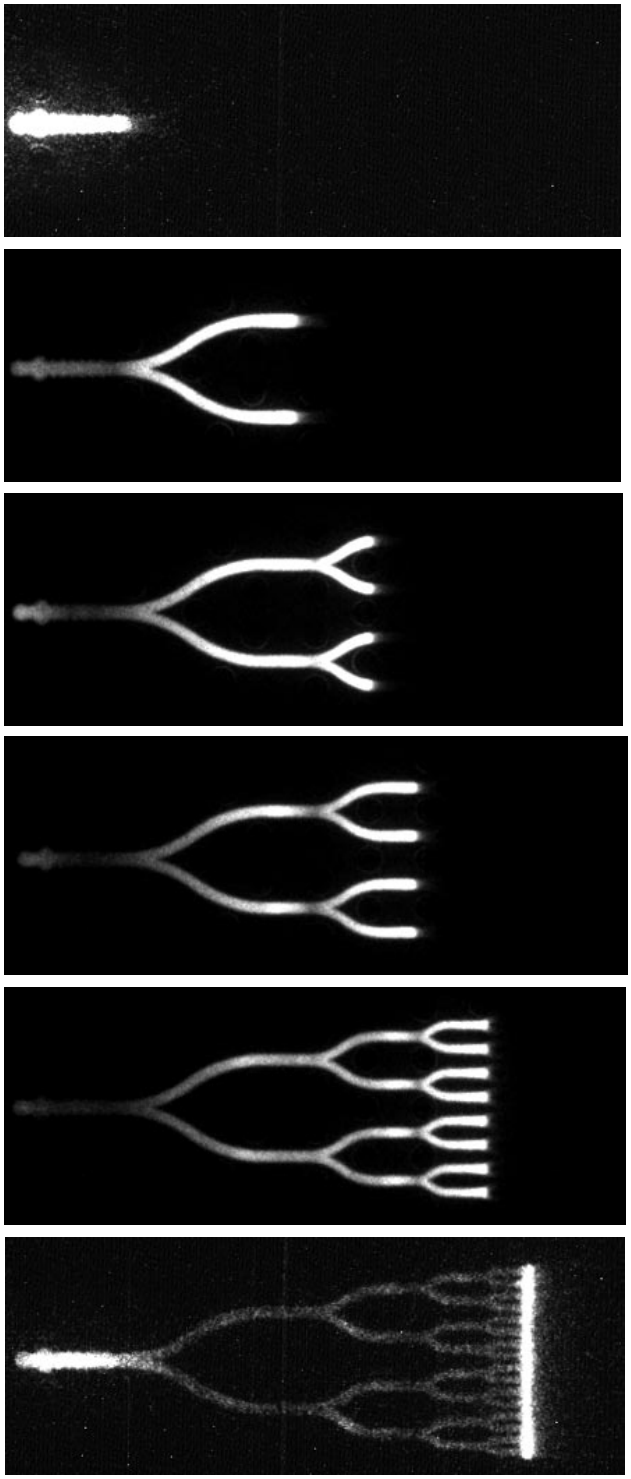

Fig. 4 Chemiluminescence imaged from the second planar initiator.

Imaging of the detonation front (Figure 7) shows a repeatable and regular collapsing circular front. The outermost black portion of the image is the initiator wall, which frames a circular testing area that is 76 mm in diameter. In each image, the innermost cir-

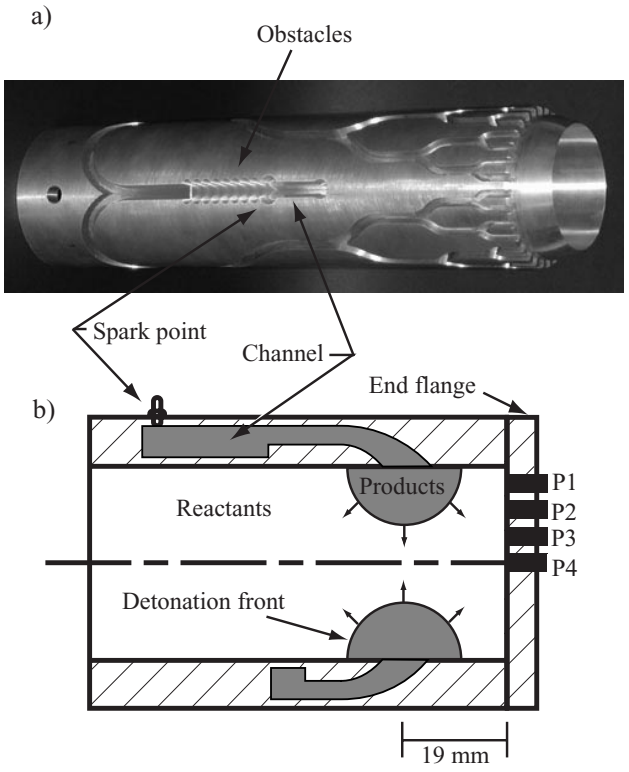

Fig. 5 The second-generation toroidal initiator a) inner sleeve and b) accompanying schematic. In the schematic, the grey areas are products and the white area is reactants. Hatched sections indicate the initiator walls. Pressure transducers located on the end flange are labeled P1, P2, P3, P4.

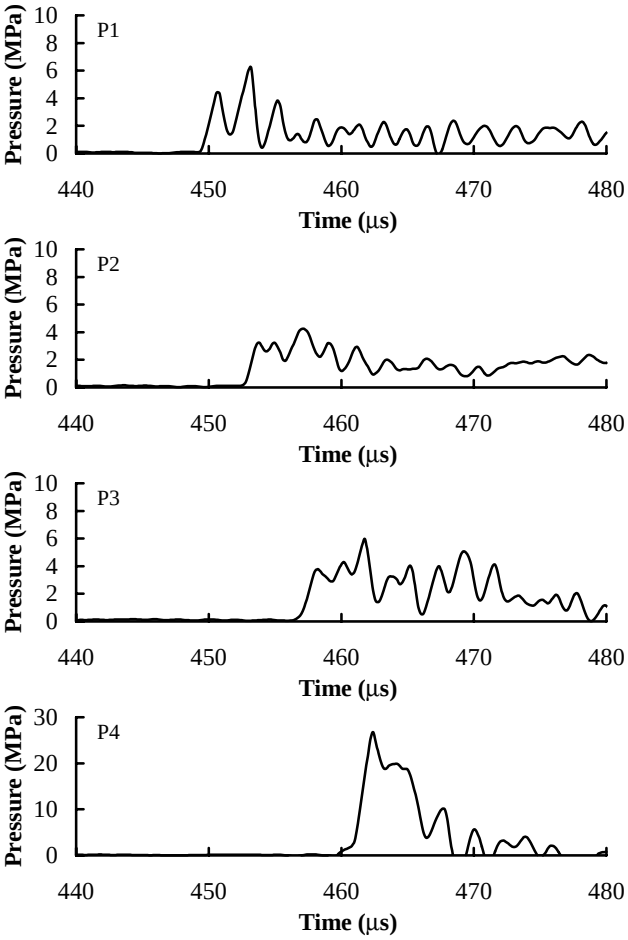

Fig. 6 A typical set of pressure traces from the toroidal initiator. Mixture was stoichiometric ethylene-oxygen at 1 bar initial pressure. For this mixture P_{CJ} = 3.4 MPa. Pressure traces correspond to locations shown in Figure 5. Time origin is at the instant the spark is fired. Note the different vertical scale on the last pressure trace (P4).

cle corresponds to the collapsing detonation front. In some images, a "flower-shaped" structure between the collapsing front and the initiator wall is visible. This structure is the interaction of the detonation with the window. In Figure 7, each image is from a separate experiment. However, multiple images of a single experiment have also been obtained using a Cordin Model 220 gated, intensified camera capable of taking an exposure every 10 ns. These images verified that with stoichiometric ethylene-oxygen mixtures at 1 bar initial pressure, the initiator operation is repeatable. These results are essentially identical to the previous results with single images from multiple experiments.

Using the series of images shown in Figure 7, it is possible to infer the wave speed of the collapsing circular front. Figure 8 contains an distance-time plot of wave radius against time. The data indicate that the wave is collapsing at a steady rate. The measured wave velocity is 2200 m/s, which is within 9% of the theoretical detonation wave speed of 2400 m/s predicted by the CJ theory. The velocity deficit can be explained by using Whitham's method to solve for the amount of overdrive present in the imploding wave. Previously,[13] we found that collapsing toroidal waves exhibit an initial period of velocity and pressure decay which is followed only by a period of over-drive due to wave focusing at the very end of the implosion process. In earlier work, velocity measurements of the collapsing wave were not available. The pressure of the imploding wave was observed to decay early on in the implosion process; however, this effect was attributed to wave decay and wall effects. The observed velocity deficit in recent experiments provides more direct evidence that the toroidal wave is under-driven for much of the implosion process.

While the device produces repeatable results with stoichiometric ethylene-oxygen mixtures, it produces irregular results with stoichiometric propane-oxygen mixtures at 1 bar initial pressure. Figure 9 shows a series of eight images taken by the previously mentioned Cordin camera during a single experiment where the initiator was filled with propane-oxygen. In these experiments, the focus of the imploding wave was not aligned with the central axis of the initiator. Further investigation showed that the focal location of the im-

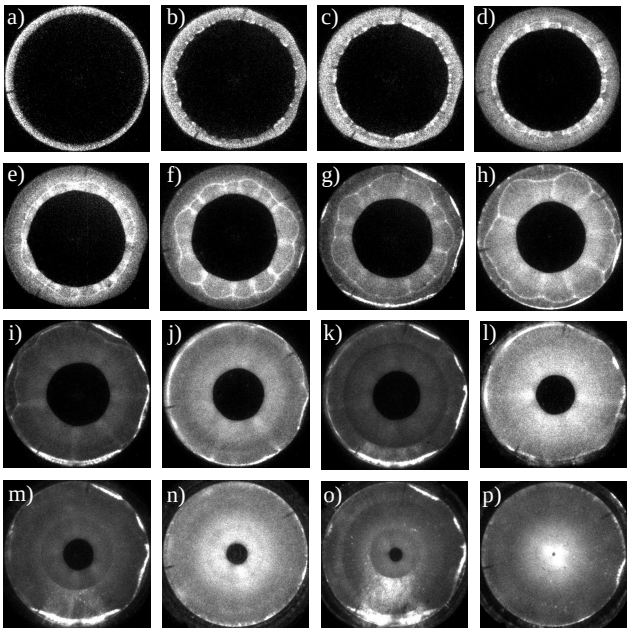

Fig. 7 Chemiluminescence images of collapsing toroidal detonation wave in a stoichiometric ethylene-oxygen mixture at 1 bar initial pressure. The period between the arrival of the detonation front at the triggering pressure transducer and imaging was a) 18 μs, b) 20 μs, c) 21 μs, d) 22 μs, e) 23 μs, f) 24 μs, g) 25 μs, h) 26 μs, i) 27 μs, j) 28 μs, k) 29 μs, l) 30 μs, m) 31 μs, n) 32 μs, o) 33 μs, p) 34 μs.

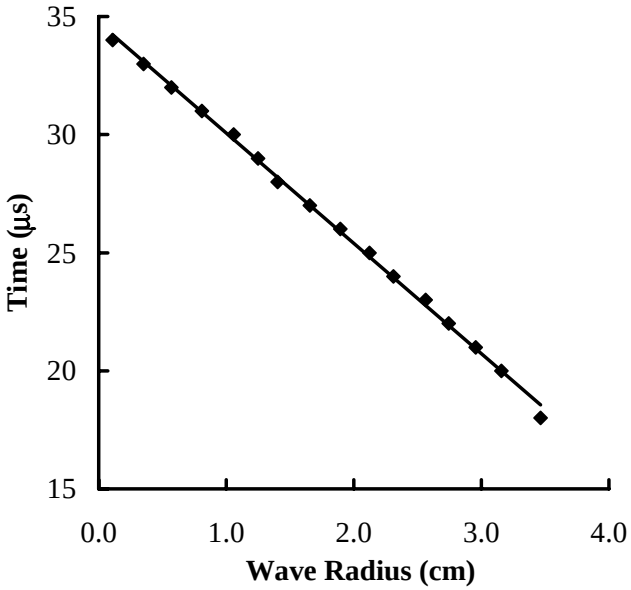

Fig. 8 A plot of wave radius as a function of time. Data is measured from the images shown in Figure 7. The slope of the line fit to the data corresponds to a velocity of 2200 m/s. The Chapman-Jouguet wave speed U_{CJ} for the mixture is 2400 m/s.

ploding wave wanders from one experiment to another. When the "off-center" focus lined up with pressure transducers along the end flange, it was apparent that the device was producing comparable pressures to tests where the focus was aligned in the center of the device. However, it is not clear at this time why the focus wanders with propane-oxygen mixtures. One possibility is that the detonation is failing in one or several of the small channels of the initiator.

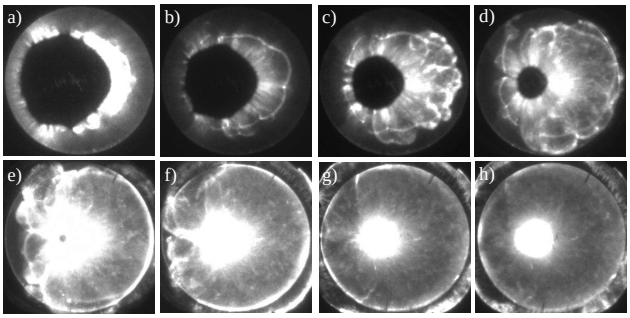

Fig. 9 Chemiluminescence images of collapsing toroidal detonation wave in a stoichiometric propane-oxygen mixture at 1 bar initial pressure. Exposure times are 800 ns. The period between the arrival of the detonation front at the triggering pressure transducer and imaging was a) 26.0 μs, b) 28.5 μs, c) 31.0 μs, d) 33.5 μs, e) 36.0 μs, f) 38.5 μs, g) 41.0 μs, h) 43.5 μs.

Initiation of Hydrocarbon-Air Mixtures

Once we were satisfied that we had a design that was capable of dynamic gas injection and creating a reliable high-pressure focal region, the toroidal initiator was then used to initiate hydrocarbon-air mixtures. The initiator was attached to a longer tube, creating a detonation tube 1 m long, with 0.4 m made up by the toroidal initiator. The detonation tube was filled with ethylene-oxygen-nitrogen and propane-oxygen-nitrogen mixtures using the method of partial pressures. As before, mixture homogeneity was accomplished by gas circulation via a bellows pump. After mixing, acetylene-oxygen mixtures were injected into the initiator using the same gas injection system used with the planar initiator. For all of the following data, the gas used was a mixture of equimolar acetylene-oxygen. Shortly after injection, 30 mJ was discharged across the spark plug. Pressure transducers and ion probes located in the toroidal initiator and test section measured the resulting combustion front. The facility is shown in Figure 10.

During testing, the amount of diluent in the detonation tube mixture and the amount of gas injected were varied. The main criterion for successful initiation of the test section (detonation tube) mixtures was that the wave speed be not more than 10% below the CJ detonation velocity U_{CJ} for the test section mixture. If this criterion was met, the peak pressure of the wave was examined to ensure that it was on the order of P_{CJ} for the test section mixture. Additionally, ion probe traces were used to verify the shock wave measured by the pressure transducers was accompanied

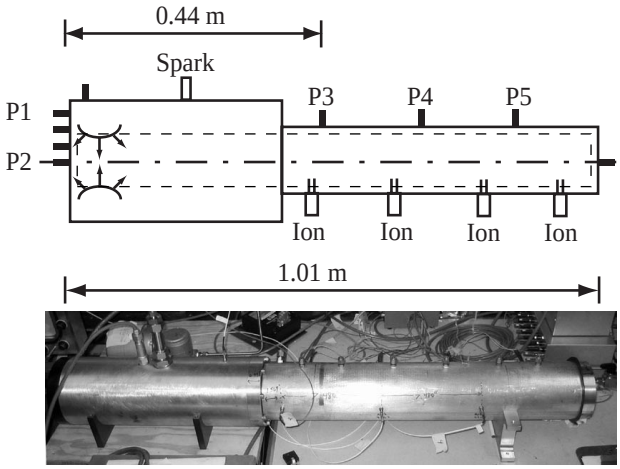

Fig. 10 A schematic and accompanying picture of the experimental setup used for initiation of hydrocarbon-air mixtures. The initiator is on the left; the detonation tube is on the right. PCBs P3-P5 are spaced 19.0 cm apart. Ion probes are spaced 15.0 cm apart.

by a tightly-coupled reaction zone. It should be noted that the measured wave speed used in the above criterion was found by averaging the wave speeds measured between P3 and P4 and between P4 and P5. (PCB locations are shown in Figure 10.)

The amount of gas used in each experiment is presented in terms of "initiator overfill." This refers to the amount of gas injected into the experiment that was in excess of the volume of the initiator. A graphical interpretation of this concept is illustrated in Figure 11. Negative values of initiator overfill correspond to the initiator not being completely filled with initiator gas. The effective volume of the initiator is 349 cc (21.6 in^3), which accounts for the actual volume of the initiator (218 cc or 13.3 in^3) and the volume of the tubing associated with the gas injection system (136 cc or 8.3 in^3). The total system volume of the initiator assembly and the attached detonation tube is 4980 cc (304 in^3). An example of overfill volume is provided for clarity: An overfill volume of 37% corresponds to the effective initiator volume in addition to 37% of the actual initiator volume:

$$21.6 \text{ in}^3 + 0.37(13.3 \text{ in}^3) = 26.5 \text{ in}^3 \ .$$

Thus, immediately after injection, the initiator is completely filled and an additional 4.9 in^3 of initiator has spilled into the main tube volume.

Examples of Pressure History and Ion Probe Data

Calibration Shot

Figure 12 shows several pressure transducer and ion probe traces from a calibration test. The location of each pressure trace is labeled and corresponds to a transducer shown in Figure 10. All ion probes were on the same data acquisition channel. It is assumed that the ion probes were triggered sequentially from left

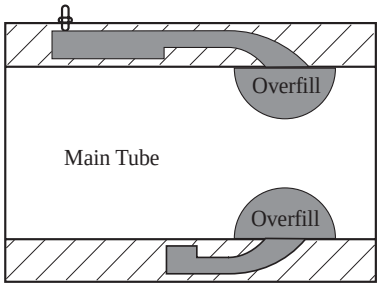

Fig. 11 The overfilled initiator gas shown as semicircular volumes in the main tube.

to right as they are shown in Figure 10. In this experiment, the test section mixture used was nitrogen. Pressure transducers 1 and 2 show data characteristic of the imploding wave and measure pressures on the order of 100 bar near the high-pressure focal region. The implosion generates a shock wave that decays as it propagates the length of the tube. The flow behind the shock wave has an overpressure of 4 bar. This overpressure agrees with the measured shock velocity corresponding to a Mach 2 shock wave. The ion probes measure no ionization as is expected from a nitrogen test mixture.

No-Go or Failed Initiation

Figure 13 shows data from a test with propane-air in the test section where a detonation was not successfully transmitted from the initiator to the test mixture. Initiator overfill in this experiment was 24% of the initiator volume. The data configuration is the same as with the previous example. Pressure transducer 1 shows a typical detonation wave which is overdriven to a very high pressure (200 bar) as it implodes near pressure transducer 2. Further down the tube, a shock wave with an overpressure of 7 bar is present. As the wave propagates the length of the detonation tube, it decays. The 7 bar overpressure is higher than the 4 bar overpressure measured in the calibration case where no combustion was present; however, it is far below the CJ pressure of 18.8 bar for stoichiometric propane-air mixtures. Inspection of the ion probe data shows the broad dips characteristic of a deflagration. Furthermore, the measured wave speeds are on the order of 800-1000 m/s, while CJ theory predicts U_{CJ} to be 1801 m/s. Thus, in this experiment, a detonation did not propagate down the length of the tube. Instead, a shock wave was present, followed by a deflagration.

Go or Successful Initiation

Data from an experiment where a propane-air test section mixture was successfully detonated are shown in Figure 14. The initiator overfill in the experiment was 37% of the volume of the initiator. The data configuration is the same as in previous examples. Pressure transducers located near the implosion focus register the same high-pressure focal region as in previous cases. This time, however, pressure transducer

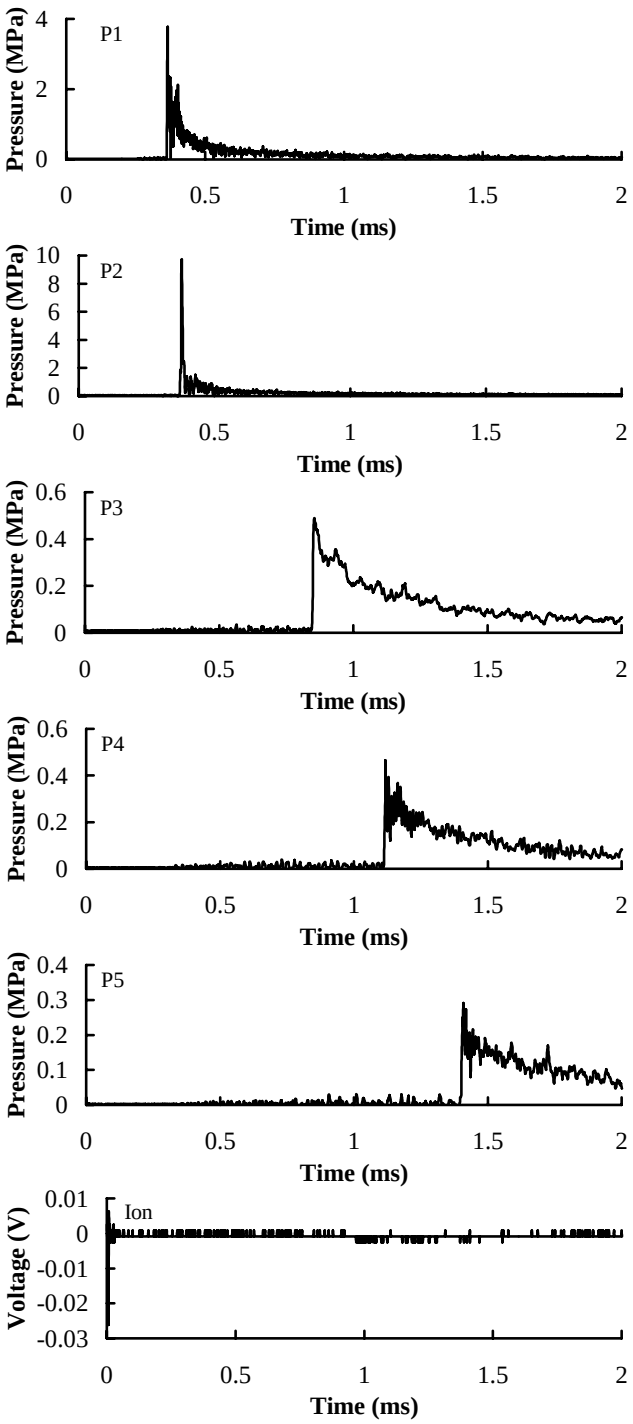

Fig. 12 Pressure and ion traces from shot 355, a typical calibration shot. Test section mixture was nitrogen at 1 bar initial pressure. Traces are labeled and correspond to locations shown in Figure 10.

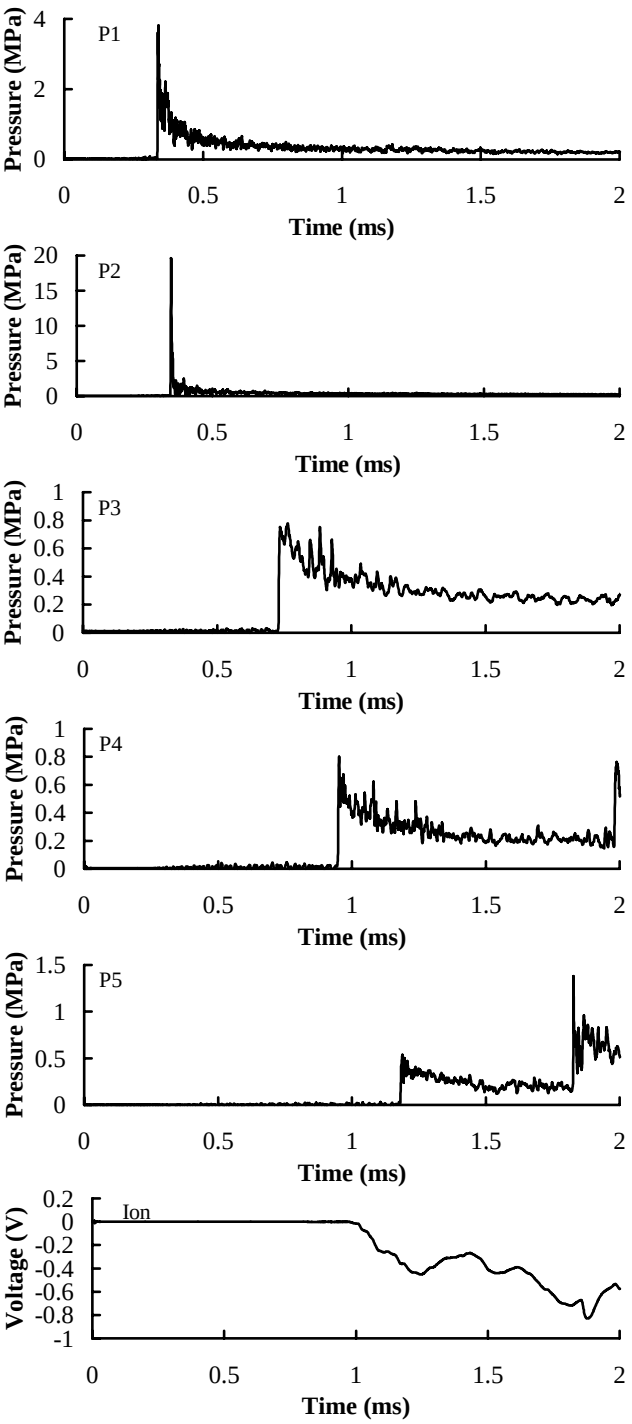

Fig. 13 Pressure and ion traces from shot 362, a typical failed initiation. Test section mixture was stoichiometric propane-air at 1 bar initial pressure. Traces are labeled and correspond to locations shown in Figure 10.

3 records the passing of a wave with an overpressure of 25 bar which is 30% above P_{CJ}. This wave maintains its overpressure as it continues to propagate the length of the tube. Measured wave speeds of 1811 m/s agree well with U_{CJ} (1801 m/s). Furthermore, the ion probe traces show the sharp spike characteristic of a detonation wave and also indicate that the combustion front is coupled with the wave.

Transmission Limits

During investigation of the transmission efficiency of the initiator, the amount of initiator gas injected into the device and the wall proximity to the implosion focus were varied. In order to vary the wall proximity to

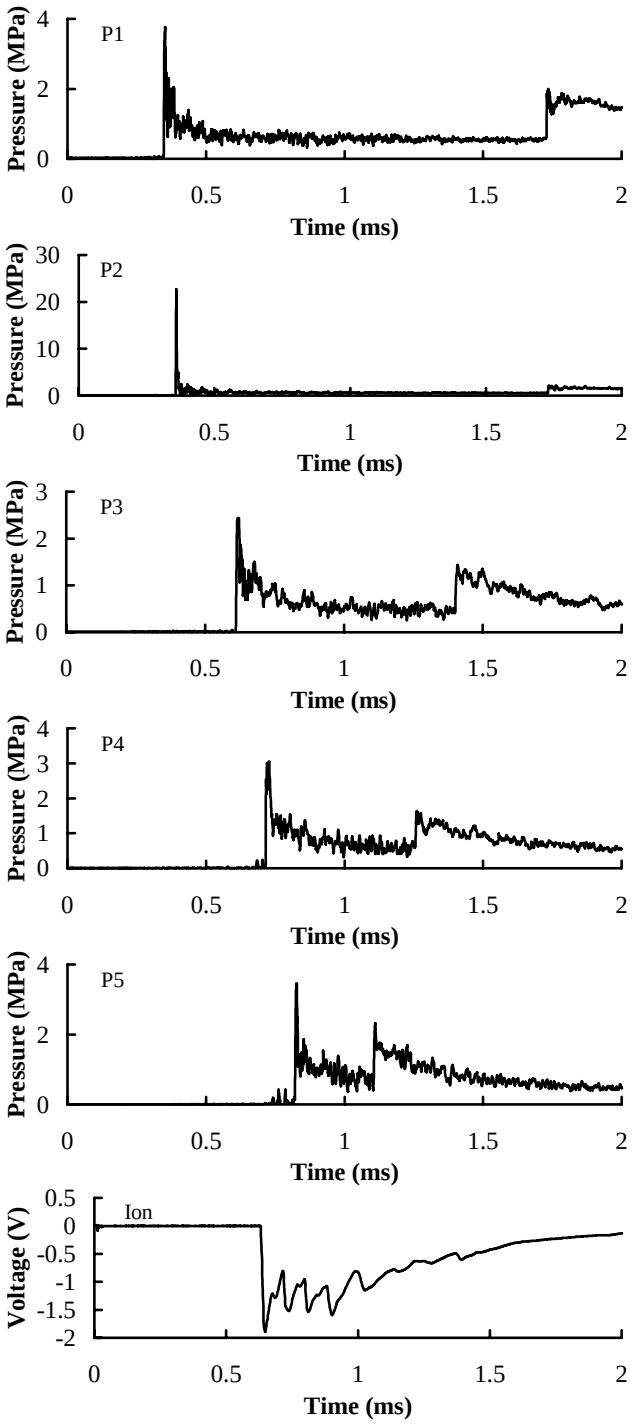

Fig. 14 Pressure and ion traces from shot 367, a typical successful initiation. Test section mixture was stoichiometric propane-air at 1 bar initial pressure. Traces are labeled and correspond to locations shown in Figure 10.

the focus, two experimental configurations were used. In the first, the focus was effectively at the end flange (Figure 15a). It was thought that the end flange would enhance the focusing by providing an additional surface to reflect the waves. In order to remove this effect, separate tests were conducted with the initiator flipped around such that the focus was about 0.4 m from the end flange (Figure 15b). In experiments with the focus at the end flange, stoichiometric propane-oxygen and ethylene-oxygen mixtures were used with varying amounts of nitrogen dilution. Experiments with no wall focusing effects involved only stoichiometric propane-air and ethylene-air mixtures. The results are separated into four categories according to wall proximity (wall focusing or no wall focusing) and fuel used in the test section (propane or ethylene).

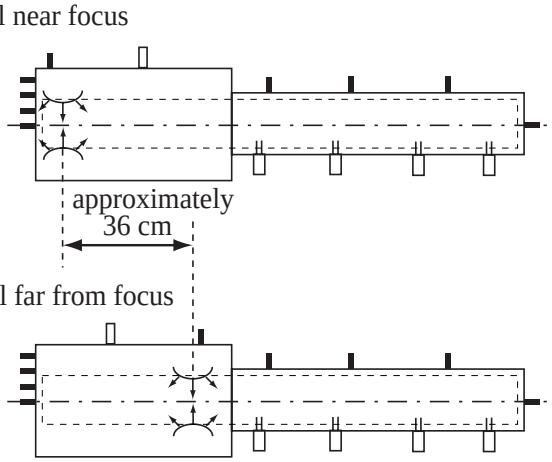

Fig. 15 Schematics illustrating the difference in the focal location of the imploding wave.

Propane Mixtures with Wall Focusing

Experimental results where the wave focus was next to the end flange wall and propane was used as fuel are shown in Table 2. The average wave velocity in the test section is compared to the amount of diluent present in the test section mixture (by mole percent). The table clearly shows that as the amount of diluent is increased, it is necessary to inject more initiator gas in order to achieve a stronger initiation event. The minimum amount of initiator gas that was able to initiate stoichiometric propane-air was found to correspond to an initiator overfill of 37%. Experiments with propane-air are presented again on a separate plot (Figure 16) in order to more clearly visualize the threshold. The wave appears to be overdriven at the critical value, hinting at the presence of a galloping wave, a phenomenon which occurs in marginal detonations. Unfortunately, velocity measurements did not have sufficient resolution and the tube was not of sufficient length to study this effect in detail. Assuming the critical amount of gas overfill was confined to a disc with the same diameter as the inside of the detonation tube (76 mm), the width of the disc would be 2.8 cm (1.1 in).

Ethylene Mixtures with Wall Focusing

Tests with ethylene fuel followed the same trend as the propane cases (Table 3); however, due to the increased sensitivity of ethylene-oxygen mixtures, much less initiator gas injection was required to initiate sto-

	Diluent (mole %)			
Initiator Overfill	50%	60%	70%	75.8%
6%	2080	940	810	X
15%	X	2000	850	X
24%	X	X	1890	840
32%	X	X	X	850
37%	X	X	X	2160
41%	X	X	X	1810
49%	X	X	X	1780
61%	X	X	X	1780
73%	X	X	X	1820

Table 2 Wave speed in the detonation tube as a function of test gas diluent and initiator overfill for stoichiometric propane-oxygen-nitrogen mixtures. The second row denotes percent moles of nitrogen in the detonation tube mixture. The first column denotes initiator overfill. All other values are wave speeds (in m/s) measured in the detonation tube. For the mixtures tested, U_{CJ} ranges from 1801 m/s (76% diluent) to 2062 m/s (50% diluent). Wave speeds above 1620 m/s can be considered detonations. If a cell is filled with "X", no experiment was performed at that condition.

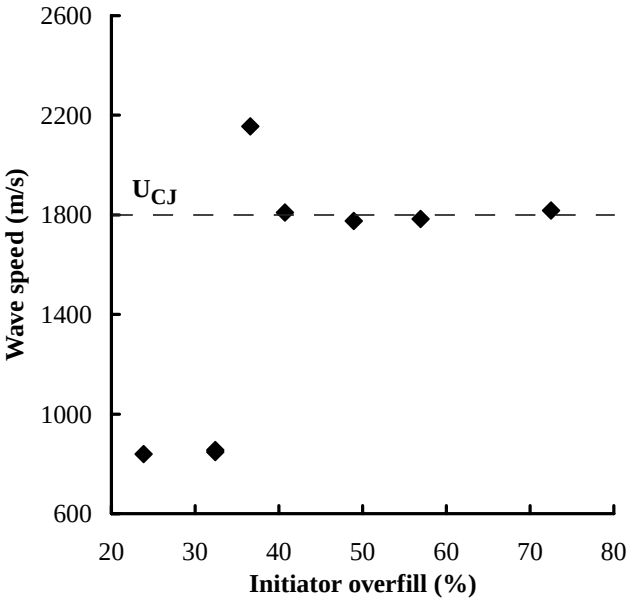

Fig. 16 Wave speed in the test mixture as a function of initiator overfill for stoichiometric propane–air mixtures. U_{CJ} is 1801 m/s.

ichiometric ethylene-air mixtures. The critical overfill value was determined to be 6%. As before, fuel-air cases are plotted alone in Figure 17. No overdriven waves are present in this case. The critical amount of overfill corresponds to a disc of diameter 76 mm and width 0.45 cm (0.18 in).

Propane Mixtures without Wall Focusing

Increasing the distance of the end flange wall from the focusing event necessitated more gas to be injected

	Diluent (mole %)			
Initiator Overfill	50%	60%	70%	73.8%
-30%	2050	1980	630	594
-7%	X	X	X	830
3%	X	X	X	850
5%	X	X	X	860
6%	X	X	X	1840
15%	X	X	X	1850
61%	X	X	X	1790

Table 3 Wave speed in the detonation tube as a function of test gas diluent and initiator overfill for stoichiometric ethylene-oxygen-nitrogen mixtures. The second row denotes percent moles of nitrogen in the detonation tube mixture. The first column denotes initiator overfill. All other values are wave speeds (in m/s) measured in the detonation tube. For the mixtures tested, U_{CJ} ranges from 1825 m/s (76% diluent) to 2060 m/s (50% diluent). Wave speeds above 1640 m/s can be considered detonations. If a cell is filled with "X", no experiment was performed at that condition.

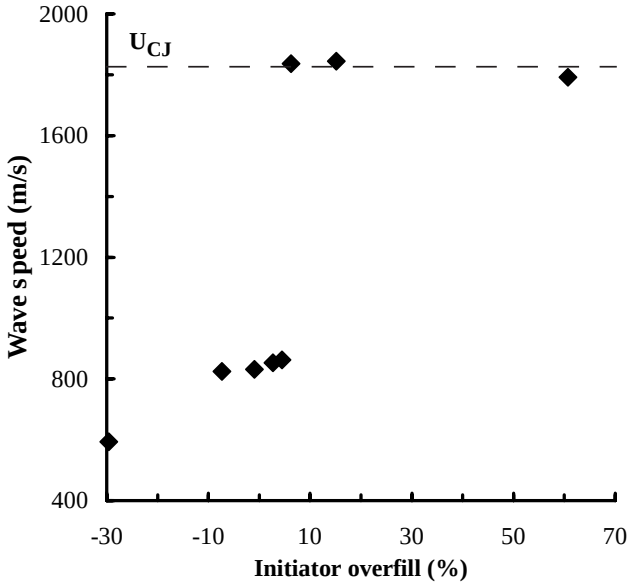

Fig. 17 Wave speed in the test mixture as a function of initiator overfill for stoichiometric ethylene-air mixtures. U_{CJ} is 1825 m/s.

to detonate propane-air mixtures. Figure 18 shows steadily increasing wave velocities as initiator overfill is increased. The critical amount of gas for initiation of the propane-air mixture was found to be 73%. It should be noted that while this is almost twice the critical overfill percent value for cases with the focus located next to the wall, twice the amount of gas was not injected. Instead, it means that twice the amount of *overfill* gas was injected. The critical amount of overfill corresponds to a disc of diameter 76 mm and a width of 5.5 cm (2.2 in).

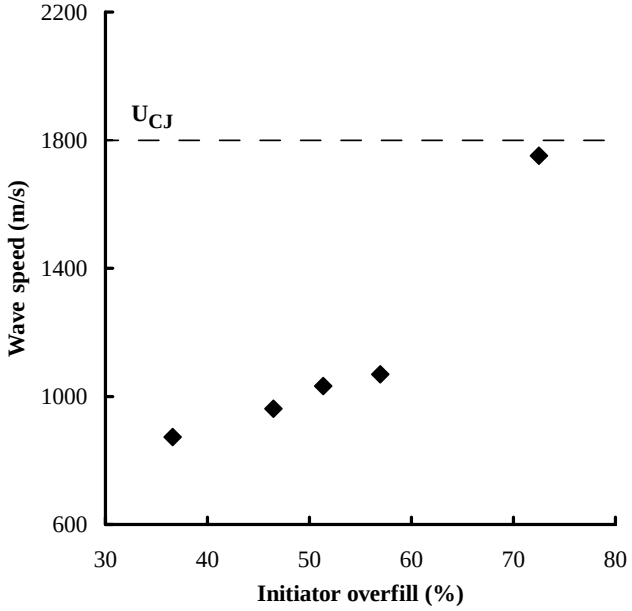

Fig. 18 Wave speed in the test mixture as a function of initiator overfill for stoichiometric propane-air mixtures with no wall effects. U_{CJ} is 1801 m/s.

Ethylene Mixtures without Wall Focusing

As with the propane cases, distancing the end flange wall from the wave focus required more gas to be injected in order to initiate the ethylene-air mixture in the test section (Figure 19). The critical amount of overfill was found to be 20%, corresponding to a disc with a diameter of 76 mm and a width of 1.5 cm (0.59 in). Table 4 summarizes the above results, comparing

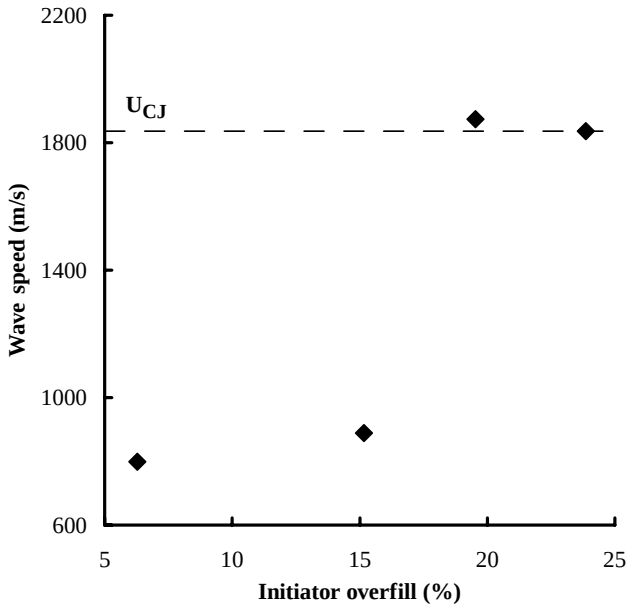

Fig. 19 Wave speed in the test mixture as a function of initiator overfill for stoichiometric ethylene-air mixtures with no wall effects. U_{CJ} is 1825 m/s.

the amount of overfill necessary for detonation transmission from the initiator to the test section with and without wall focusing for different fuels. Table 5 contains the length of the tube that the total amount of gas used in the entire initiation process would fill, were it injected directly into the detonation tube (Figure 20), as would be done with a simple tube initiator.

	With wall	No wall
C_3H_8–air	37%	73%
C_2H_4–air	6%	20%

Table 4 Critical amount of overfill necessary for detonation initiation with different experimental configurations.

	With wall	No wall
C_3H_8–air	9.3 cm	11.0 cm
C_2H_4–air	7.8 cm	8.5 cm

Table 5 Length of 76 mm tube that would be filled by critical amount of initiator gas were the gas injected directly into the tube as is shown in Figure 20.

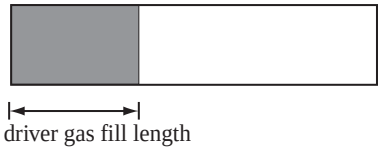

Fig. 20 Accompanying schematic for Table 5, where critical amount of initiator gas (colored grey) is injected into the detonation tube directly.

Initiation Attempts Using a Collapsing Shock Wave

The initiator was also used to generate an imploding shock wave in an attempt to initiate the test section mixture. Recent computational simulations[18] have suggested that it is possible to initiate JP10-air mixtures using impulsively started jets of JP10 and air to create an annular shock wave.

A preliminary investigation of this notion was examined by conducting imploding shock experiments with the present setup. In order to generate an imploding shock wave, the initiator was partially filled (roughly 30%–40%) with initiator gas. Detonation of this gas propagated a shock wave through the channels of the device, trailed by a deflagration. This shock wave then implodes at the focus creating an imploding annular shock wave in the fuel-air mixture.

This technique was found to not be successful at initiating stoichiometric ethylene-air mixtures. Pressure traces from an experiment where 41% of the initiator was filled with initiator mixture are shown in Figure 22. The location of the pressure and ion probe traces from Figure 22 are shown in the schematic in Figure 21. The test section mixture was ethylene-air.

Pressure transducer 2 shows a shock wave with an overpressure of 12 bar that is propagated into the mixture from the initiator. As this wave implodes, the

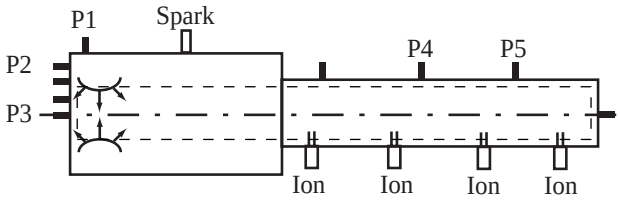

Fig. 21 A schematic of the experimental setup used for attempted initiation of hydrocarbon-air mixtures using an imploding shock wave.

pressure measured near the focus is 100 bar. Further down the tube, pressure transducers 4 and 5 show a shock with an overpressure of 4 bar. Measured wave speed in the test section is roughly 630 m/s while U_{CJ} is 1825 m/s. Thus, initiation of the test section mixture was not successful. In fact, the pressure traces are similar to those previously presented for the "failed initiation" case where an imploding detonation wave (instead of a shock wave) was propagated into the test section. It appears that, in these experiments, the imploding shock wave was not of sufficient Mach number and the post-shock flow was not of sufficient duration to initiate the ethylene-air mixture. Further study is needed to determine the critical parameters for initiation in this configuration. Key issues relevant in initiation are discussed in the next section.

Key Concepts in Initiation

Review of literature on initiation of gaseous detonations identifies three main techniques currently used to detonate mixtures: direct initiation via a blast wave, DDT, and use of tube initiators. The following will briefly review each technique, focusing on the efficiency of the method at initiating detonations inside a tube. The ideas behind the design of the toroidal initiator will then be discussed and its operational efficiency will be compared to the previously mentioned methods of initiation.

Direct Initiation

In direct initiation, rapid energy deposition into a mixture (e.g. via an exploding wire or high explosive) generates a strong blast wave. For a given mixture, sufficiently strong blast waves evolve into a detonation wave. Blast waves that are too weak evolve into an expanding, decaying shock wave trailed by a slower, decoupled deflagration.

Early work by Zeldovich et al.[19] proposed that in order for the blast wave to successfully initiate a detonation in a mixture, adequate time must be available for the shocked gas to release its chemical energy. The most basic consideration is that the shocked gas must be hot enough to release the chemical energy sufficiently rapidly behind the shock. The decay rate of the blast wave is also very important. If the blast wave decayed too rapidly, the chemical reactions would be "turned off" resulting in failure to initiate a detonation. If the blast wave was of insufficient Mach number, the chemical kinetics would never be "turned on" in the first place. Direct initiation studies since then have focused on using a blast wave or shock to generate high temperatures and pressures in the test mixture for an extended duration. In chemical terms, this translates to maintaining minimum values of the

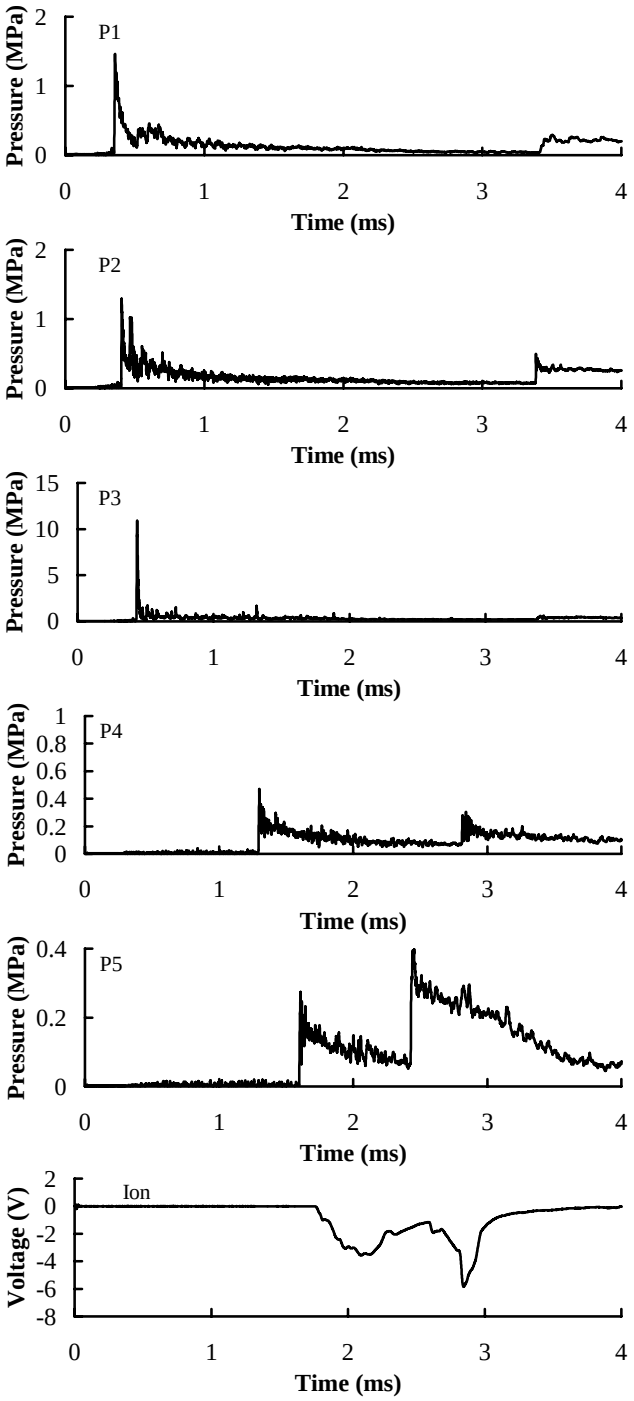

Fig. 22 Pressure and ion traces from shot 382, a typical shock initiation experiment. Test section mixture was stoichiometric ethylene-air at 1 bar initial pressure. Traces are labeled and correspond to locations shown in Figure 21.

key reaction rates for a sufficient length of time that the chain-branching reactions can build a sufficient radical pool to create a self-sustaining reaction-shock wave system.

Zeldovich chose the induction time τ as the key time scale and suggested that, for successful initiation, the time for the blast wave to decay from its initially overdriven state to below the CJ Mach number M_{CJ} be longer than the CJ induction time. From this assumption, he was able to show that the critical energy E_c to directly initiate a spherical detonation wave was dependent on the cube of the CJ induction time

$$E_c \sim \tau_{CJ}^3 \ . \tag{1}$$

Subsequently, there have been a number of studies that have examined this issue from an experimental[20,21] and numerical[22] point of view. Comparison of empirical models with the data by Benedick et al.[21] showed agreement with the "surface energy model"[23]

$$E_c \cong 430\,\rho_0\,U_{CJ}^2\lambda^3 \ . \tag{2}$$

Theoretical and numerical analyses[22] of blast wave initiation with simplified kinetic models lead to a similar expression, but with the reaction zone length Δ_* instead of cell width

$$E_c \cong B\,\rho_0\,U_*^2\theta^3\Delta_*^3 \tag{3}$$

where U_* is a critical shock velocity that is slightly lower than the CJ value. The value θ is the reduced activation energy

$$\theta = \frac{E_a}{\tilde{R}T_s} \tag{4}$$

where $\tilde{R}$ is the universal gas constant and T_s is the post-shock temperature. Eckett et al.[22] showed that this model was in reasonable quantitative agreement with experimental H_2-air, C_2H_4-air and CH_4-O_2-N_2 direct initiation data.

It is also worth noting that most comparisons[21,22,24] between theory and experimental work have been done for spherical initiation. Limited comparison[14] between theory and experiment has been done for the planar and cylindrical geometries due to lack of experimental data. Critical energy required for initiation of mixtures of interest is discussed at the end of this section.

Tube Initiator

A tube initiator has a smaller diameter than the main tube and is filled with a more sensitive mixture. Usually, low-energy ignition and DDT is used to create a detonation that propagates out into a larger main tube filled with the mixture to be detonated. The initiation mechanism is similar to that of direct initiation described previously: A shock wave created by diffraction of the detonation out of the tube initiator into the mixture raises the mixture temperature for a sufficient length of time in order to successfully initiate the mixture. In tube initiators that are closed at one end, the Taylor wave is responsible for the decay of temperature and pressure behind the shock or detonation wave. The Taylor wave is the expansion wave which brings the shocked gas to rest and originates due to boundary conditions at the closed end of the tube initiator. Thus, the arrival of the Taylor wave into the main tube can be delayed by extending the length of the tube initiator. This would allow the mixture in the main tube more time to release its chemical energy after it was processed by the shock wave. In addition, the pressure decay due to diffraction and pressure increases due to reflection may play a significant role in initiator operation.

Kuznetsov et al.[25] conducted experimental and numerical studies in an effort to correlate the transmitted wave overpressure and duration to the critical limits of initiation. They identified the ratio of the time of the arrival of the Taylor wave to the chemical time scale of the mixture to be initiated as a key factor in tube initiator effectiveness. The other important factor was the overpressure of the shock wave transmitted into the test section by the tube initiator. The results show that as initiator length is increased, the overpressure of the transmitted wave can be decreased to a lower limit and successful initiation can still occur. The critical overpressure of the transmitted wave increases with decreasing initiator length implying that a higher reaction rate is necessary to initiate in a shorter time. Murray et al.[3] have also recognized this effect and used experimental data to identify initiator length, transmitted wave overpressure, and initiator diameter as the key parameters in initiation. They found the same relationship as Kuznetsov et al. and also showed that increasing initiator diameter decreases the necessary initiator length.

In addition to generating a blast wave, tube initiators also take advantage of the proximity of the tube walls to enhance detonation transmission. The shock wave diffracting into the test section reflects off the tube walls and generates regions of higher temperature and pressure than would occur were the tube walls not present. Often, the temperature and pressure in these regions is high enough to create a detonation kernel which then spreads throughout the tube. The result is that tube initiators are able to initiate less sensitive mixtures than can be done using spherical initiation due to this shock reflection effect.

Experiments[26] in hydrogen-containing mixtures have established critical Mach numbers for the shock waves propagating into the test section that predict if and how initiation will occur with tube initiators. Transmitted shocks with Mach numbers greater than 1.4 are expected to cause ignition near obstacles or tube walls. Shock waves with Mach numbers between

1.2 and 1.4 could cause flame ignition in reflections from obstacles or walls. Shock Mach numbers less than 1.2 are not thought to cause flame ignition, even when reflected off the tube walls or obstacles.

Murray et el.[12] were able to enhance the transmission efficiency of a tube initiator by placing a circular blockage plate at the exhaust of the tube initiator. As the shock wave diffracted around the blockage plate, a focus was generated along the central axis of the tube just downstream of the blockage plate, resulting in a region of high energy density that facilitated detonation re-initiation. Using this technique, Murray et al. were able to successfully transmit the detonation to the test section using tube initiators with diameters 2.2 times smaller than the critical diameter necessary for tube initiators with simple circular orifices.

Deflagration-to-Detonation Transition

DDT provides another mechanism for detonation initiation. During DDT, a weak flame or deflagration is accelerated by promoting turbulence at the flame front, often by placing obstacles in the flame path. Turbulence wrinkles the flame front and increases its surface area. This increase in surface area results in a higher energy release rate and sends compression waves ahead of the deflagration which coalesce into a shock. A positive feedback mechanism exists such that the leading shock is strengthened by the compression wave sent from the trailing deflagration. The shocked fluid is then raised to a high temperature, accelerating combustion and compression wave generation.

Onset of detonation is characterized by the generation of hot spots or local explosions that occur when a pocket of unburned gas located between the leading shock and a trailing turbulent flame brush suddenly explodes. This explosion generates a hot spot that enables a fast flame to couple to the shock front, resulting in a detonation. Hot spots have been found to be key in the DDT process.

Studies of DDT carried out at McGill University[27,28] in tubes with obstacles have determined that at the optimum blockage ratio $BR = 0.43$, the tube inner diameter d must be greater than the cell size of the mixture λ for a mixture to successfully undergo DDT in the tube. Subsequent work[29–31] has confirmed that the ratio d/λ must be near or above 1. Dorofeev et al.[32] note that the variations of this ratio can range from 0.8 to 5.1 depending on the blockage ratio.

Dorofeev et al.[32] have examined DDT phenomenon over a wide range of length scales and various mixtures in order to develop scaling parameters that characterize the onset of detonation. In particular, they suggest that the minimum distance[32] L for detonation formation is dependent on the cell size of the mixture such that

$$L = 7\lambda\,. \tag{5}$$

For propane-air mixtures with cell sizes of 50 mm, this suggests a characteristic length L of 350 mm as the minimum length necessary for DDT to occur. However, this criterion appears to be necessary but not sufficient for the onset of detonation. Higgens et al.[33] showed that even by enriching stoichiometric propane-air mixtures with oxygen and acetylene, the DDT distance could not be reduced to less than 1.5 m. Minimum DDT lengths of 1.5 m are impractical. Caltech has also done previous work[34] studying DDT for use with ethylene-air mixtures in short length tubes (less than 1 m) and found the DDT length was too long to use DDT alone as an initiation system.

Common Themes

Direct initiation illustrates the importance of increasing the chemical reaction rate of the mixture to be initiated above a minimum value for a requisite length of time. In geometries with confining walls, tube initiators have been shown to be more effective at initiating detonations by utilizing shock reflection off walls to generate localized regions of high temperature (hot spots) that are capable of initiating detonations. In less sensitive mixtures, these hot spots do not directly initiate the mixture, but accelerate the DDT process. Recent research[6,13,35] has focused on developing and enhancing the strength of these hot spots in an effort to initiate detonations in less sensitive mixtures.

The toroidal initiator attempts to improve on previous initiation methods by directly creating a hot spot by using an imploding wave to generate a volume of shock heated gas with a high temperature core. It is expected that the size of the volume of gas and the temperature distribution inside this volume are directly dependent on the success of the concept. However, the focal region of the toroidal initiator has not yet been characterized. Instead, the toroidal initiator will be compared to other previously discussed initiator designs in order to evaluate its performance. The critical energy required for initiation of spherical and planar waves is compared to the energy content of the gas used in the toroidal initiator. The performance of the toroidal initiator is also compared to that of a model tube initiator by comparing initiation energy, as well as amounts of fuel and oxygen used.

Comparison with Spherical Initiation Energy

Spherical initiation involves creating a spherically expanding strong shock by releasing energy in a concentrated form (i.e. sparks or high explosives). This also provides a possible method to establish a detonation inside a tube since spherically-initiated waves will eventually evolve into quasi–planar waves at large distances from the initiation source. A critical amount of energy is required in order for the shock wave to develop into a spherically-expanding detonation front.

Radulescu[14,36] has developed a model for predicting critical initiation energies of a mixture for three

different geometries. The model, outlined below, is based on the similarity solution for a strong blast wave in a non–reacting medium and uses criteria developed by Zeldovich[19] and Lee[20] as well as experimental results.[21]

The classic similarity solution for a strong blast wave propagating through a non–reacting mixture with specific heat ratio γ is

$$E_s = \alpha_j \left(\frac{j+2}{2}\right)^2 \gamma\, P_0 M_s^2 R_s^j \tag{6}$$

where α_j is a constant obtained from blast wave theory ($\alpha_1 = 1.009$, $\alpha_2 = 0.986$, $\alpha_3 = 0.851$). The parameter j denotes the geometry of the wave where $j = 1$, 2, 3 for planar, cylindrical, and spherical geometries, respectively. Dimensional analysis indicates that the units of the source energy term are geometry-dependent: Planar waves have source energy terms in units of energy per area; cylindrical wave source terms are in units of energy per length; spherical source terms have units of energy. The parameters γ and P_0 are determined from the initial conditions of the mixture.

Zeldovich proposed that the critical energy for initiation was derived from a blast wave of sufficient Mach number (M_s^*) and sufficient duration, or in this model, sufficient distance (R_s^*). Radulescu[14] notes that observations of the minimum shock Mach number that is sufficient to initiate detonation has been found to be $0.5 M_{CJ}$ and uses this as the critical shock Mach number value M_s^*.

Research[37,38] in fuel-air mixtures has shown that for spherical initiation geometries,

$$R_s^* \approx 10\lambda \tag{7}$$

is the critical distance at which detonation occurs. In order to determine the critical distance R_s^* for other geometries, a length scale related to blast wave decay is introduced. In order to do this, the explosion length[20]

$$R_0 = \left(\frac{E_j}{P_0}\right)^{1/j} \approx \text{const} \tag{8}$$

associated with the critical source energy is assumed to be invariant. Solving for the energy yields

$$E_j = R_0^j\, P_0\ . \tag{9}$$

It is possible to relate the critical energies from the three different geometries by taking the ratio of energies of different geometries

$$R_0 = \frac{E_{j+1}}{E_j} = \frac{E_{spherical}}{E_{cylindrical}} = \frac{E_{cylindrical}}{E_{planar}}\ . \tag{10}$$

Critical radii can be determined by substituting E_s in Eqn. 6 into the energies for the different geometries in Eqn. 10 and assuming typical values of $\gamma = 1.4$, $M_{CJ} = 5.5$ (typical of hydrocarbon-air mixtures), and thus $M_s^* = 0.5 M_{CJ} \approx 2.8$. Resulting radii are

$$R^*_{cylindrical} \approx 0.59 R^*_{spherical} \approx 0.59\,(10\lambda) \approx 5.9\lambda\ , \tag{11}$$

$$R^*_{planar} \approx 0.16 R^*_{spherical} \approx 1.6\lambda\ . \tag{12}$$

Thus, it is possible to estimate the critical energy for any mixture and geometry as long as the cell size and CJ Mach number are known. Table 6 summarizes the above results for spherical and planar detonations.

	Spherical	Cylindrical	Planar
j	3	2	1
R_s^*	10λ	5.9λ	1.6λ
M_s^*	$0.5 M_{CJ}$	$0.5 M_{CJ}$	$0.5 M_{CJ}$
$E_c/\gamma P_0 M_{CJ}^2$	$1330\lambda^3$	$34.3\lambda^2$	$0.91\ \lambda$
E^*_{s,C_3H_8-air}	701.5 kJ	361.8 kJ/m	192.0 kJ/m^2

Table 6 Critical detonation parameters for different geometries from Radulescu.[14] The bottom row shows the critical energy for a stoichiometric propane-air mixture with P_0 = 1 bar, M_{CJ} = 5.49, λ = 50 mm, and γ = 1.4.

Radulescu observes that the critical energy estimate for spherical geometries agrees well with experimentally determined values[21] for ethylene-air mixtures at atmospheric conditions. However, the predicted critical energy for stoichiometric propane-air mixtures at 1 bar initial pressure and 295 K initial temperature shown in Table 6 is more than twice the experimentally measured value[39] of 283 kJ. Radulescu also notes that it is difficult to check the validity of the model for planar detonations since there is little experimental data available on critical energies for this geometry. The toroidal initiator has been found to use a 434 cc (26.5 in^3) volume of equimolar acetylene-oxygen gas initially at a temperature of 295 K and a pressure of 1 bar to initiate a planar detonation in a tube filled with stoichiometric propane-air. The effective heat of reaction Δh^0 of the initiator gas mixture was calculated using the perfect gas, 2–γ, CJ detonation model from Thompson[40]

$$\Delta h^0 = R_{CJ} T_{CJ} \left(\frac{\gamma_{CJ}}{\gamma_{CJ}-1}\right)\left(1+\frac{\gamma_{CJ}-1}{2}\right) - R_0 T_0 \left(\frac{\gamma_0}{\gamma_0-1}\right)\left(1+\frac{\gamma_0-1}{2} M_{CJ}^2\right)\ . \tag{13}$$

STANJAN[41] is used to perform the equilibrium calculations necessary to obtain the CJ Mach number and specific heat ratio. For acetylene-oxygen mixtures, the effective heat of reaction is shown in Figure 23 as a function of equivalence ratio ϕ. For the equimolar (ϕ = 2.5) mixtures used in the toroidal initiator, the effective heat of reaction was determined to be Δh^0 =

7.07 MJ/kg of initiator mixture. Thus, the energy released by detonation of the initiator gas mixture was found to be

$$E_{toroidal} = \Delta h^0 \, \rho_0 \, V_{initiator} = 3.62 \text{ kJ} . \quad (14)$$

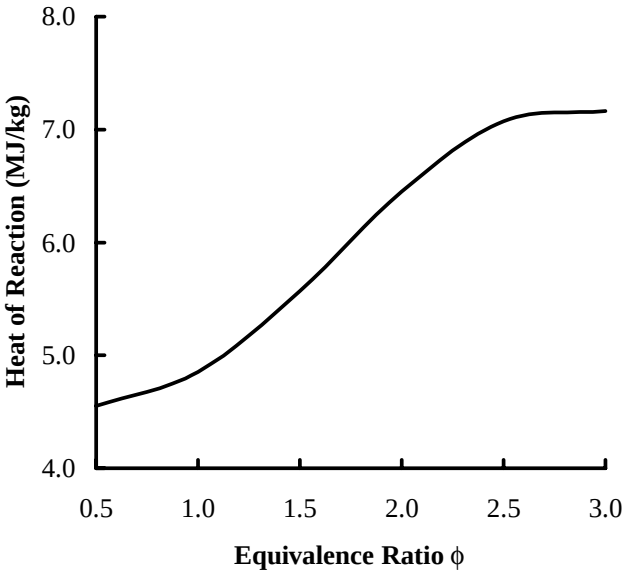

Fig. 23 Effective heat of reaction of acetylene-oxygen mixtures as a function of equivalence ratio.

Table 7 contains the critical energies of the toroidal initiator, predicted by the Radulescu model and from spherical initiation experiments. All table entries are normalized by the critical toroidal initiation energy (3.62 kJ). Thus, the normalized entries represent a sort of efficiency factor. It is clear that spherical initiation is far less efficient than the toroidal initiator. This is expected, however, as spherical initiation is intended to initiate a spherical detonation in an open space, while the toroidal initiator initiates a planar detonation wave in a 76 mm diameter tube.

Toroidal	Spherical (predicted)	Spherical (exp)	Planar (predicted)
3.62 kJ	701.5 kJ	283.0 kJ	0.87 kJ

Table 7 Critical energies for spherical and planar initiation compared to the toroidal initiator.

Comparison with Planar Initiation Energy

The energy required to initiate a planar detonation wave provides a more useful comparison with the toroidal initiator critical energy as both initiation schemes generate a nominally planar detonation wave in a 76 mm diameter tube. As previously determined, the toroidal initiator uses 3.62 kJ of energy to initiate stoichiometric propane-air mixtures.

Using the modified blast wave model, the critical planar initiation energy per unit area was previously found to be 192.0 kJ/m^2. Thus, the critical planar initiation energy required to initiate a planar detonation in a 76 mm diameter tube with a cross-sectional area of

$$A_{tube} = \pi \frac{d^2}{4} = 4.54 \times 10^{-3} \text{ m}^2 \quad (15)$$

is 192.0 kJ/m^2 $\times$ $(4.54 \times 10^{-3}$ m$^2) = 0.87$ kJ. As with the critical spherical energies, Table 7 compares the critical planar initiation energy to the critical toroidal initiation energy. The critical energy predicted for planar initiation appears to be a quarter of the critical toroidal initiation energy. Unfortunately, experimental measurements of planar initiation energy are not available for comparison.

Comparison with a Typical Tube Initiator

Recent work by Murray et al.[3] has resulted in a model based on an extensive data set that is capable of predicting the necessary tube initiator dimensions for stoichiometric acetylene-oxygen initiator mixtures. The model predicts that for a tube initiator diameter to main tube diameter ratio of $d_d/d = 0.5$, the tube initiator length L_d necessary to initiate a stoichiometric propane-air test section mixture with a cell size of $\lambda = 50$ mm (2 in) is approximately $L_d/\lambda = 9$ or L_d = (45.7 cm) 18 in. For main tube diameter of $d = 76$ mm (3 in) used in the toroidal initiator experiments, this corresponds to a tube initiator volume of

$$V_d = \frac{\pi d^2}{4} L_d \quad (16)$$

$$= \frac{\pi \left(0.75\lambda\right)^2}{4} 9\lambda \quad (17)$$

$$\approx 4\lambda^3 \quad (18)$$

$$= 32 \text{ in}^3 \text{ or } 524 \text{ cc} \quad (19)$$

Since the Murray et al. model assumes a stoichiometric acetylene-oxygen initiator gas, the effective heat of reaction of the mixture using the perfect gas, 2–γ, CJ detonation model is found to be $\Delta h^0 = 4.85$ MJ. This corresponds to an energy release of

$$E_{d,uncorr} = \Delta h^0 \, \rho_0 \, V_{d,uncorr} \quad (20)$$

$$= 3.14 \text{ kJ} . \quad (21)$$

The amount of oxygen necessary for successful initiation is important in performance modeling as oxygen tanks will result in payload losses. The masses of fuel and oxygen initiator gas were also calculated and are shown in Table 8. Examination of the amount of initiator gas used by each initiator reveals that the toroidal initiator uses more fuel, but about half the amount of oxygen used by the model tube initiator.

Summary and Conclusion

A detonation wave initiator has been developed which is capable of producing a large-aspect ratio planar detonation wave in a less sensitive mixture. The

	Toroidal Initiator	Tube
Energy	3.62 kJ	3.14 kJ
mass C_2H_2	0.23 g	0.16 g
mass O_2	0.28 g	0.49 g

Table 8 Critical values for a model tube initiator compared to the toroidal initiator.

planar initiator uses a single weak spark and a small amount of fuel-oxygen mixture to produce the planar wave in a short distance.

A toroidal initiator has been developed which creates an imploding wave in an insensitive mixture using a small amount of fuel-oxygen gas and a weak spark. The imploding detonation wave initiates detonations in propane-air and ethylene-air mixtures. Imploding shock waves (instead of detonation waves) were not found to initiate the fuel-air mixtures for the single case tested.

The performance of this toroidal initiator was compared to other initiation techniques such as direct initiation in spherical and planar geometries and diffraction from a tube initiator. The initiator was found to use on the order of 100 times less energy than spherical initiation to detonate the propane-air mixtures in a detonation tube. The predicted energy necessary for direct initiation of a planar detonation inside of a tube was a quarter of the critical toroidal initiation energy. However, no experimental data were available to validate the predicted planar detonation initiation energy.

The tube initiator is probably the most useful comparison case as extensive experimental and numerical data are available. Furthermore, tube initiators are currently used on operational pulse detonation engines. The toroidal initiator and tube initiator were found to use similar amounts of energy to detonate propane-air mixtures. In the case examined, the tube initiator was found to be more fuel efficient, while the toroidal initiator was found to be more oxygen efficient. It is expected that the amount of oxygen used by initiation systems is an important measure of performance as the oxygen will be carried on-board with the pulse detonation engine, resulting in performance losses. Future work will focus on reducing the amount of fuel used for initiation and investigate the effectiveness of the toroidal initiator when used with propane-oxygen and ethylene-oxygen initiator mixtures. Fundamental studies on the mechanism of initiation near the wave focus are also in progress.

Acknowledgment

The authors would like to thank J. Haggerty and B. St. John for their expertise and patience during initiator construction. They are also grateful to F. Pintgen for conducting the water visualization experiments and to N. Nebeker and P. Nagel at Cordin Scientific Imaging for use of their Model 220 CCD camera.

This work was supported by the Office of Naval Research Grant *Pulse Detonation Engines: Initiation, Propagation and Performance* (Dept. of Navy Grant number N00014-02-1-0589, subcontract PY-1905), General Electric contract GE-PO A02 81655 under DABT-63-0-0001, and the Department of Defense and Army Research Office through a National Defense Science and Engineering Graduate Fellowship.

References

[1]Brophy, C. M. and Netzer, D. W., "Effects of Ignition Characteristics and Geometry on the Performance of a JP-10/O_2 Fueled Pulse Detonation Engine," 35th AIAA/ASME/SAE/ASEE Joint Propulsion Conference and Exhibit, June 20–24, 1999, Los Angeles, CA, AIAA 99-2635.

[2]Brophy, C., Sinibaldi, J., and Damphousse, P., "Initiator Performance for Liquid–Fueled Pulse Detonation Engines," 40th AIAA Aerospace Sciences Meeting and Exhibit, January 14–17, 2002, Reno, NV, AIAA 02-0472.

[3]Murray, S., Zhang, D., and Gerrard, K., "Critical Parameters for Pulse Detonation Engine Pre-detonator Tubes," *International Colloquium on the Dynamics of Explosions and Reactive Systems*, Hakone, Japan, July 27 - August 14-7 2003.

[4]Whitham, G., "On the propagation of shock waves through regions of non-uniform area or flow," *Journal of Fluid Mechanics*, Vol. 4, 1958, pp. 337–360.

[5]Lee, J. and Lee, B., "Cylindrical Imploding Shock Waves," *The Physics of Fluids*, Vol. 8, No. 12, 1965, pp. 2148–2152.

[6]Jiang, Z. and Takayama, K., "Reflection and focusing of toroidal shock waves from coaxial annular shock tubes," *Computers and Fluids*, Vol. 27, No. 5-6, 1998, pp. 553–562.

[7]Takayama, K., Kleine, H., and Gronig, H., "An Experimental Investigation of the Stability of Converging Cylindrical Shock Waves in Air," *Experiments in Fluids*, Vol. 5, No. 5, 1987, pp. 315–322.

[8]Devore, C. and Oran, E., "The Stability of Imploding Detonations in the Geometrical Shock Dynamics (CCW) Model," *Physics of Fluids*, Vol. A4, No. 4, 1992, pp. 835–844.

[9]Oran, E. and Devore, C., "The Stability of Imploding Detonations - Results of Numerical Simulations," *Physics of Fluids*, Vol. 6, No. 1, 1994, pp. 369–380.

[10]Terao, K., Akaba, H., and Shiraishi, H., "Spherically imploding detonation waves initiated by 2-step divergent detonation," *Shock Waves*, Vol. 4, No. 4, 1995, pp. 187–193.

[11]Akbar, R., *Mach Reflection of Gaseous Detonations*, Ph.D. thesis, Rensselaer Polytechnic Institute, Troy, New York, 1997.

[12]Murray, S., Thibault, P., Zhang, F., Bjerketvedt, D., Sulmistras, A., Thomas, G., Jenssen, A., and Moen, I., "The Role of Energy Distribution on the Transmission of Detonation," *Proceedings of the International Colloquium on Control of Detonation Processes*, Moscow, Russia, July 4-7, 2000.

[13]Jackson, S. and Shepherd, J., "Initiation Systems for Pulse Detonation Engines," 38th AIAA/ASME/SAE/ASEE Joint Propulsion Conference and Exhibit, July 7–10, 2002, Indianapolis, IN, AIAA 2002-3627.

[14]Radulescu, M., *Experimental Investigation of Direct Initiation of Quasi-Cylindrical Detonations*, Master's thesis, McGill University, Montreal, Canada, 1999.

[15]Hill, L., private communication, 2000.

[16]Grunthaner, M., Jackson, S., and Shepherd, J., "Design and Construction of an Annular Detonation Initiator," GALCIT Technical Report 2001.005, Graduate Aeronautical Laboratories, California Institute of Technology, Pasadena, CA 91125, 2001.

[17]Austin, J., *The Role of Instability in Gaseous Detonation*, Ph.D. thesis, California Institute of Technology, Pasadena, CA, 2003.

[18]Chiping, C. and Kailasanth, K., "Detonation Initiation in Pulse Detonation Engines," 41st AIAA Aerospaces Sciences

Meeting and Exhibit, January 6–9, 2003, Reno, NV, AIAA 2003-1170.

[19]Zel'dovich, I., Kogarko, S., and Simonov, N., "An Experimental Investigation of Spherical Detonation of Gases," *Soviet Phys - Tech Phys*, Vol. 1, 1956, pp. 1689–1713.

[20]Lee, J. and Matsui, H., "A Comparison of the Critical Energies for Direct Initiation of Spherical Detonations in Acetylene-Oxygen Mixtures," *Combust. Flame*, Vol. 28, 1977, pp. 61–66.

[21]Benedick, W., Guirao, C., Knystautas, R., and Lee, J., "Critical Charge for the Direct Initiation of Detonation in Gaseous Fuel-Air Mixtures," *Prog. Astro. Aero.*, Vol. 106, 1985, pp. 181–202.

[22]Eckett, C., Quirk, J., and Shepherd, J., "The Role of Unsteadiness in Direct Initiation of Gaseous Detonations," *Journal of Fluid Mechanics*, Vol. 421, 2000, pp. 147–183.

[23]Lee, L., Knystautas, R., and Guirao, C., *Proceedings of the First Specialist Meeting on Fuel–Air Explosions*, University of Waterloo Press, Waterloo, Canada, 1982.

[24]Vasilev, A., "Gaseous Fuels and Detonation Hazards," *28th International Conference of ICT*, Karlsruhe, Germany, June 1997.

[25]Kuznetsov, M., Dorofeev, S., Efimenko, A., Alekseev, V., and Breitung, W., "Experimental and Numerical Studies on Transmission of Gaseous Detonation to a Less Sensitive Mixture," *Shock Waves*, Vol. 7, No. 5, 1997, pp. 297–304.

[26]Breitung, W., Chan, C., Dorofeev, S., Eder, A., Gelfand, B., Heitsch, M., Klein, I., Malliakos, A., Shepherd, J., Studer, E., and Thibault, P., "Flame Acceleration and Deflagration to Detonation Transition in Nuclear Safety," State-of-the-Art Report by a Group of Experts NEA/CSNI/R(2000)7, OECD Nuclear Energy Agency, August 2000.

[27]Peraldi, O., Knystautas, R., and Lee, J., "Criteria for Transition to Detonation in Tubes," *The 22nd International Symposium on Combustion*, Pittsburgh, PA, USA, 1988, pp. 1629–1637.

[28]Guirao, C., Knystautas, R., and Lee, J., "A summary of hydrogen–air detonations for reactor safety." Report NUREG/CR-4961, Sandia National Laboratories/McGill University, Montreal, Canada, 1989.

[29]Lee, J., Knystautas, R., and Chan, C., "Turbulent Flame Propagation in Obstacle-Filled Tubes," *Proceedings of the 20th Symposium (International) on Combustion*, Pittsburgh, PA, USA, 1984, pp. 1663–1672.

[30]Teodorczyk, A., Lee, J., and Knystautas, R., "Propagation Mechanism of Quasi-detonations," *Symp. Int. Combust. Proc.*, 1988, pp. 1723–1731.

[31]Kuznetsov, M., Alekseev, V., and Dorofeev, S., "Comparisons of Critical Conditions for DDT in Regular and Irregular Cellular Detonation Systems," *Proceedings of the 22nd ISSW*, London, England, 1999, p. 180.

[32]Dorofeev, S., Sidorov, V. P., Kuznetzov, M. S., Matsukov, I. D., and Alekseev, V. I., "Effect of Scale on the Onset of Detonations," *Shock Waves*, Vol. 10, 2000.

[33]Higgins, A., Yoshinaka, P., and Lee, J., "Sensitization of Fuel-Air Mixtures for Deflagration to Detonation Transition," *Proceedings of the International Colloquium on Control of Detonation Processes*, Moscow, Russia, July 4-7, 2000.

[34]Cooper, M., Jackson, S., Austin, J., Wintenberger, E., and Shepherd, J. E., "Direct Experimental Impulse Measurements for Detonations and Deflagrations," *Journal of Propulsion and Power*, Vol. 18, No. 5, 2002, pp. 1033–1041.

[35]Gelfand, B., Khomik, S., Bartenev, A., Medvedev, S., Gronig, H., and Olivier, H., "Detonation and Deflagration Initiation at the FOcusing of Shock Waves in a Combustible Mixture," *Shock Waves*, Vol. 10, 2000, pp. 197–204.

[36]Radulescu, M., Higgins, A., Murray, S., and Lee, J., "An Experimental Investigation of the Direct Initiation of Cylindrical Detonations," *Journal of Fluid Mechanics*, Vol. 480, 2003, pp. 1–24.

[37]Elsworth, J., Shuff, P., and Ungut, A., "Galloping Gas Detonations in the Spherical Mode," *Prog. Astro. Aero.*, Vol. 94, 1984, pp. 130–150.

[38]Bull, D., Elsworth, J., and Hooper, G., "Initiation of Spherical Detonation in Hydrocarbon/Air Mixtures," *Acta Astro*, Vol. 5, 1978, pp. 997–1008.

[39]Kaneshige, M. and Shepherd, J., "Detonation Database," Tech. Rep. FM97-8, Graduate Aeronautical Laboratories, California Institute of Technology, 1997.

[40]Thompson, P., *Compressible–Fluid Dynamics*, McGraw–Hill, New York, 1988.

[41]Reynolds, W. C., "The Element Potential Method for Chemical Equilibrium Analysis: Implementation in the Interactive Program STANJAN, Version 3," Tech. rep., Dept. of Mechanical Engineering, Stanford University, Stanford, CA, January 1986.